PERGAMON

Scripta Materialia 46 (2002) 425–429

Scripta MATERIALIA

www.actamat-journals.com

Fracture toughness of snow in shear and tension

H.O.K. Kirchner [a], G. Michot [b], J. Schweizer [c,*]

[a] Institut de Sciences des Matériaux, Bat. 410, Université Paris-Sud, F-91405 Orsay Cedex, France
[b] Laboratoire de Physique des Matériaux, Ecole des Mines, Parc de Saurupt, F-54042 Nancy Cedex, France
[c] Swiss Federal Institute for Snow and Avalanche Research, Flüelastrasse 11, CH-7260 Davos Dorf, Switzerland

Received 9 October 2001; accepted 20 December 2001

Abstract

Snow slab avalanche release involves brittle fracture. The fracture criterion in mixed mode for dry snow ($\rho = 170$ kg m^{-3}) was determined by cantilever beam experiments: $(K_{\mathrm{Ic}}^2 + K_{\mathrm{IIc}}^2)^{1/2} = 430 \pm 90$ Pa m$^{1/2}$. Fracture toughness in shear, K_{IIc}, is about the same as in tension, K_{Ic}.

Keywords: Mechanical properties; Brittle fracture; Fracture toughness; Snow slab avalanche

1. Introduction

As brittle fracture leads to slab avalanche release, fracture toughness is an essential property of snow to be considered for snow slab stability evaluation [1]. Recently Louchet [2] and Kirchner [3] have proposed release scenarios, and the fracture toughness of snow in tension has been determined [4]. Fracture in tension can occur at the top margin of a snow slab avalanche preceded by a shear fracture in the weak layer or at the weak interface underlying the slab [5]. The fracture toughness in shear, K_{IIc}, is therefore of particular interest. In fact, mixed mode situations, where the snow slab is under both shear and tension are likely to exist. It is therefore necessary to measure not only K_{Ic} and K_{IIc} separately, but to establish a fracture criterion for mixed mode. Generally speaking, K_{IIc} of any material has rarely ever been measured. In practice pure tensile and shear loadings are rare, mixed mode loadings prevail. In the laboratory it is notoriously difficult to subject specimens to pure traction or pure shear [6–9].

2. Test geometry and data

The standard four point shear specimen of Richard et al. [7,8,10] has been modified to allow for mixed mode. The reason for using the cantilever beam geometry of Fig. 1 is its simplicity. Scaled down versions could be used for in situ measurements in the field. Measurement of the fracture toughness is reduced to measurement of length and weight. Beams of height $w = 20$ cm and width $t = 10$ cm are cantilevered by $L = 10$ cm, and a weight P is applied at a distance $H = 5$ cm to the side of the crack. With a fishing line a crack of

* Corresponding author. Tel.: +41-81-417-0164; fax: +41-81-417-0110.
E-mail address: schweizer@slf.ch (J. Schweizer).

1359-6462/02/$ - see front matter
PII: S1359-6462(02)00007-6

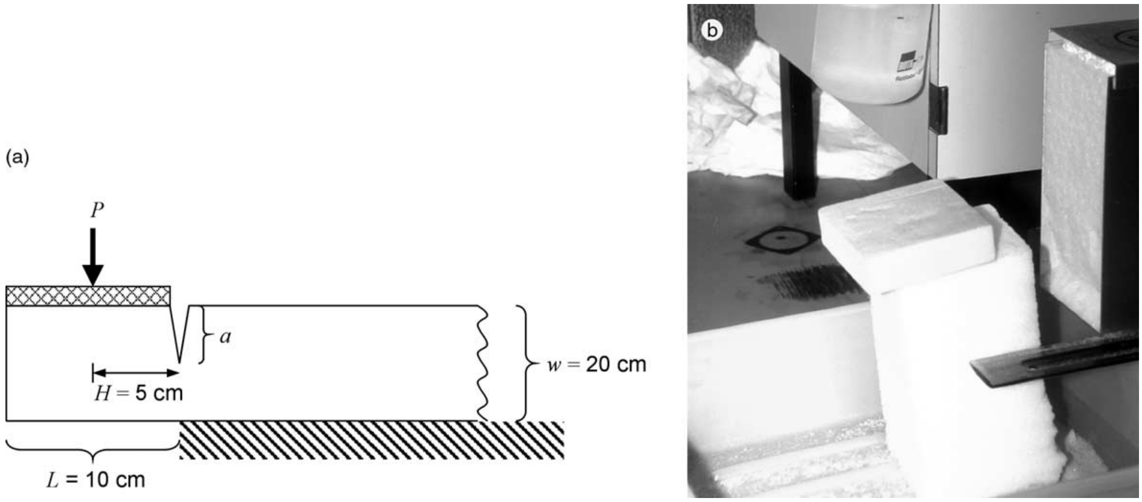

Fig. 1. Specimen geometry used. The load P is applied 5 cm to the left of the crack in the cantilever beam of height $w = 20$ cm and thickness $t = 10$ cm. (a) schematic and (b) photograph of experimental set-up after fracture has occurred.

depth a is cut into the beam along the plane of support. The resulting notch is narrower than the grain size of snow. Since any crack in snow will be intergranular rather than intragranular, the cuts are representative for natural cracking in snow.

On 11 January, 2001 a set of 18 such beams were tested at a temperature of -20 ± 1 °C in the cold laboratory of the Swiss Federal Institute for Snow and Avalanche Research SLF. The snow had been harvested the day before, and stored overnight at -20 °C in the cold laboratory. The snow originated from a layer of recently deposited snow, was characterised according to [11] as decomposing and fragmented precipitation particles and small rounded grains of 0.3–0.8 mm in size; snow hardness index was estimated as 1–2, and snow density was 170 ± 10 kg m^{-3}. In situ temperature at the time of harvesting was -9 °C. In order to further characterize the snow texture, samples were preserved and subsequently analysed with the surface section technique (Fig. 2). The high porosity of low density snow

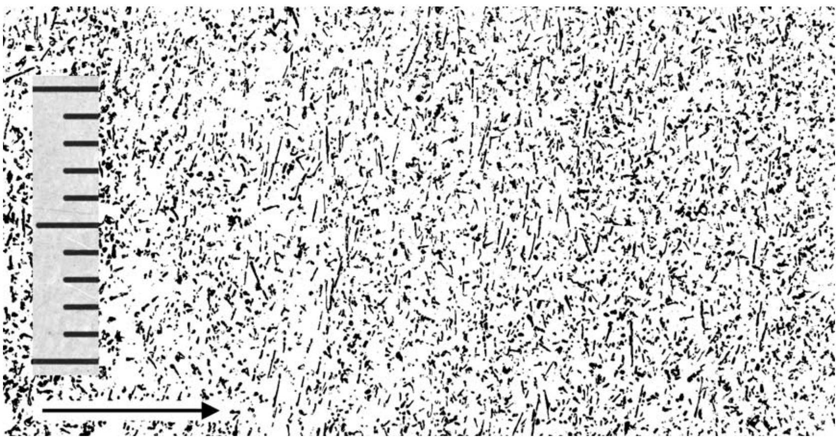

Fig. 2. Microstructure of snow type tested. Binarized picture of a surface section. Black denotes ice, white is pore space ($\rho = 174$ kg m^{-3}). Scale given is 1 cm. Arrow points to snow surface (right margin was parallel to snow surface, as were top of beams).

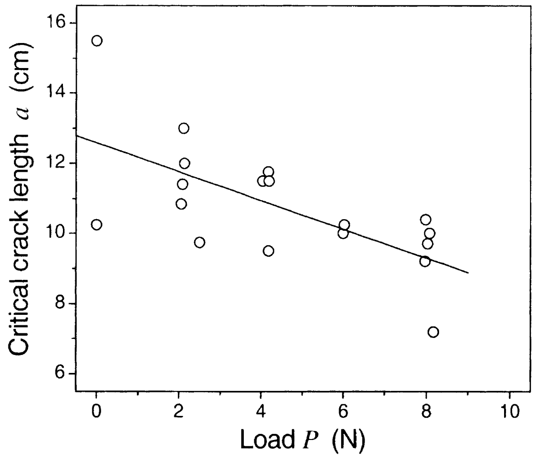

Fig. 3. The critical crack length a as a function of the applied load P. The linear trend, decreasing crack length a with increasing load P, is statistically highly significant.

that typically forms slab avalanches, is well illustrated.

Fig. 3 shows the crack length a at which the overhanging part of the beams broke off as a function of the applied load P. The scatter in crack length a for one and the same load P is not only due to experimental difficulties, but genuine and well known for the case of snow [12]. This is due to the fact that failure of snow, in particular in the brittle range, is not of deterministic but statistical nature [13,14]. Under identical experimental conditions, the low Weibull modulus of snow makes fracture a haphazard affair.

3. Stress intensities

Our geometry (Fig. 1) resembles the geometry of Fig. 4, for which formulae are available. In addition to the applied load P, the weight of the cantilever G acts as body force and creates a moment M. For each experiment, G ($\approx$3.4 N) was determined by weighing the part of the snow beam that was broken off. Combination of the pure bending case 2.13 of Tada et al. [15] and the four point shear case 10.15 of Murakami [16] provides

$$K_{\mathrm{I}} = \left\{ F_{\mathrm{I}}\left(\frac{P+G}{wt}\right) + F\left(\frac{6M}{w^2}\right) \right\} \sqrt{\pi a}, \tag{1}$$

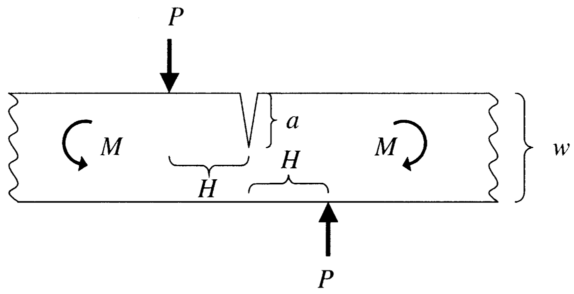

Fig. 4. The geometry for which analytical expressions (Eqs. (1) and (2)) are available.

$$K_{\mathrm{II}} = F_{\mathrm{II}}\left(\frac{P+G}{wt}\right)\sqrt{\pi a}. \tag{2}$$

The geometric factors used, F_{I}, F_{II}, and F are shown in Fig. 5 [15,16]. Because of the difference between our geometry (Fig. 1) and the one used for the finite element calculations [15] (Fig. 4), the values are only approximate. The values of F_{II} in Fig. 5 agree, up to 10%, with the value for $H/w = 0.5$ for the compact shear case 10.12 of Murakami [16], and thus seem sufficiently reliable.

Certainly, F_{II} and F increase, and F_{I} decreases with crack length; also the absolute values are correct up to factor of two. In any case, both F_{II} and $\sqrt{a}$ vary little, the range of K_{II} covered by our measurements comes from the variation of the load P.

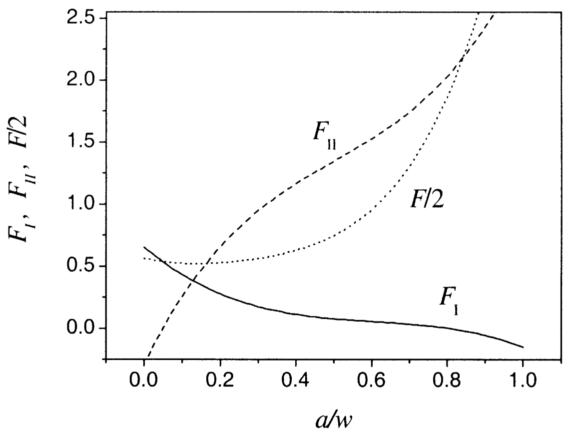

Fig. 5. Geometric factors (Eqs. (1) and (2)) as a function of the relative crack length a/w.

If the cantilever is long and the cut short, $a < w$, the second term in Eq. (1) becomes dominant. In that situation $6FMt > F_{II}(P + G)w$, so that $K_I > K_{II}$. This was the case for the previous K_I measurements [4]. The opposite extreme, a short cantilever under external load, favours mixing and is the geometry used. Eqs. (1) and (2) are based on the assumptions of beam theory. Accordingly, in the un-cracked beam, the tensile stress varies linearly, and the shear stress parabolically across the profile [10]. For short beams and shear loading this is only approximately true [17]. Since our geometry is likely to become standard, calibration curves for K_I and K_{II} need to be determined. For pure body loading these will be linear in the density and function of (a/w) and (L/w). For the case of external loading they will be linear in P and functions of (a/w), (L/w) and (H/w).

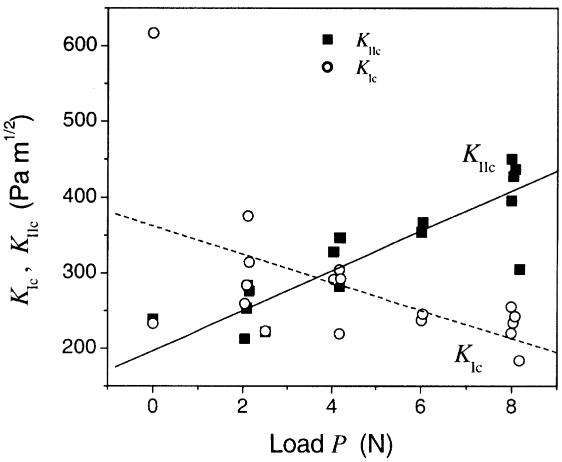

Fig. 6. The fracture toughness in tension, K_{Ic} and in shear, K_{IIc} as a function of the applied load P. The linear trends shown are statistically significant.

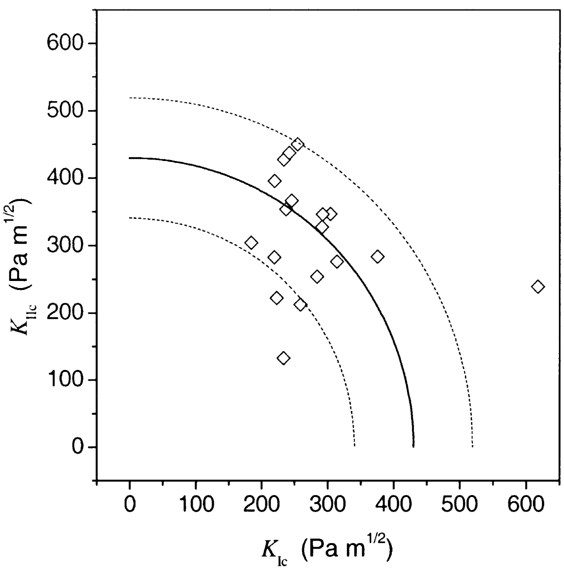

Fig. 7. Stress intensities K_{Ic} and K_{IIc} at which snow fractures in mixed mode. Mean values of the toughness, irrespective of mixing, are $K_{Ic} = 280 \pm 95$ Pa m$^{1/2}$ and $K_{IIc} = 310 \pm 85$ Pa m$^{1/2}$. In mixed mode, as indicated by concentric circles, the criterion is $(K_{Ic}^2 + K_{IIc}^2)^{1/2} = 430 \pm 90$ Pa m$^{1/2}$.

4. Results and discussion

The weight of the snow creates a moment $M = 1.73\ \mathrm{N\,m^{-1}}$ in the crack plane. Given the fact that for the resulting $6M/w^2 = 260$ Pa, that for loads P between 20 and 80 $\mathrm{N\,m^{-1}}$ the factor $(P + G)/wt$ varies between 270 and 570 Pa, and that the geometric factor $F_I \ll F$ (Fig. 5), one concludes that in Eq. (1) the first term is small compared to the second one. Physically, this means that to K_I only the weight of the snow, but not the external load P contributes, while to K_{II} the load P contributes. This way the mixing K_I/K_{II} can be controlled (Fig. 6).

From the data of Fig. 3 we computed the stress intensities according to Eqs. (1) and (2). As the applied load P increases, the critical crack length a decreases, but K_{II} increases. On the other hand, K_I decreases with decreasing crack length a. The tensile and shear components are out of phase, with increasing loading the mixing changes: shear mode increases, tension mode decreases. In Fig. 7 the stress intensities at which the snow breaks in mixed mode is shown. What is approximately conserved, and this is an experimental result, is the amplitude:

$$\sqrt{K_{Ic}^2 + K_{IIc}^2} = 430 \pm 90\ \mathrm{Pa\,m^{1/2}}. \tag{3}$$

This result is reasonable: in mode I two surfaces of energy γ are created by the crack extension force

K_{Ic}^2/E, thus one should have $2\gamma = K_{\mathrm{Ic}}^2/E$, where E is Young's modulus, about 0.5 MPa for the type of snow tested [18]. With $K_{\mathrm{Ic}} = 250\ \mathrm{Pa\,m^{1/2}}$ one obtains $\gamma = 63\ \mathrm{mJ\,m^{-2}}$. The surface energy of snow has never been measured. A simple model of an open-cell foam [19] with beams of thickness t and length L gives

$$\frac{\gamma_{\mathrm{snow}}}{\gamma_{\mathrm{ice}}} = 4(t/L)^2 = 4\frac{\rho_{\mathrm{snow}}}{\rho_{\mathrm{ice}}} = 0.74. \tag{4}$$

In fact, Petrenko and Withworth [20] report the surface free energy of ice at 0 °C to be about 70 $\mathrm{mJ\,m^{-2}}$, compatible with our results considering the simple foam model used.

The critical size a_{c} of a crack under shear stress τ in a material of toughness K_{IIc} is given by

$$\tau\sqrt{\pi a_{\mathrm{c}}} = K_{\mathrm{IIc}}. \tag{5}$$

A snow slab of density ρ and thickness h on a slope of angle α exerts a shear stress

$$\tau = \tfrac{1}{2}\rho g h \sin 2\alpha. \tag{6}$$

For typical values, $\rho = 170\ \mathrm{kg\,m^{-3}}$, $h = 0.5$ m and $\alpha = 38°$, Eq. (5) provides a critical crack size $a_{\mathrm{c}} = 0.1$ m. This is in accordance with previous estimates of the critical size of an imperfection needed to initiate fracture propagation in snow slab avalanche release [21]. In snow slab avalanche release, however, the faces of the shear crack are pressed together by the weight of the snow. The relevant K_{II} under such friction is presumably larger than our values measured with open frictionless surfaces [22].

5. Conclusions

The fracture toughness of snow in shear, K_{IIc}, is about the same as the fracture toughness of snow in tension, K_{Ic}. For snow of density 170 $\mathrm{kg\,m^{-3}}$, the fracture criterion in mixed mode is $(K_{\mathrm{Ic}}^2 + K_{\mathrm{IIc}}^2)^{1/2} = 430 \pm 90\ \mathrm{Pa\,m^{1/2}}$. With its extraordinary low values of K_{Ic} and K_{IIc} snow is one of the most brittle materials known to man. Nevertheless, fracture mechanics is applicable and is the theory appropriate for catastrophic failure of snow slopes. Snow slab avalanche release models should reflect this fact.

Acknowledgements

We would like to thank Georges Krüsi for preparing the surface section sample.

References

[1] McClung DM. J Geophys Res B 1981;86(11):10783.
[2] Louchet F. Ann Glaciol 2001;32:285.
[3] Kirchner HOK. In: Bouchaud E, Jeulin D, Prioul C, Roux S, editors. Physical aspects of fracture. Dordrecht: Kluwer; 2001. p. 47.
[4] Kirchner HOK, Michot G, Suzuki T. Phil Mag A 2000;80:1265.
[5] McClung DM, Schaerer P. The avalanche handbook. Seattle: The Mountaineers; 1993.
[6] Anderson TL. Fracture Mechanics. Boca Raton: CRC Press; 1995.
[7] Richard HA, Tenhaeff D, Hahn HG. Materials Park, OH: ASM 8517-023; 1986.
[8] Richard HA, Tenhaeff D, Hahn HG. In: Brown MW, Miller KJ, editors. Biaxial and multiaxial fatigue. London: Mech Eng Publ; 1989. p. 217.
[9] Parker AP. The mechanics of fracture and fatigue. London: Spon; 1981.
[10] He MY, Hutchinson JW. J Appl Mech 2000;67:207.
[11] Colbeck C, Akitaya E, Armstrong R, Gubler H, Lafeuille J, Lied K, McClung DM, Morris E. The international classification for seasonal snow on the ground. Wallingford, Oxon: International Association of Scientific Hydrology, International Commission on Snow and Ice; 1990.
[12] Schweizer J. Ann Glaciol 1998;26:97.
[13] Michot G, Kirchner HOK. Phil Mag A, submitted for publication.
[14] Michot G, Kirchner HOK. Scripta Mater, submitted for publication.
[15] Tada H, Paris PC, Irwin GR. The stress analysis of cracks handbook. New York: ASME Press; 2000.
[16] Murakami Y, editor. Stress intensity factors handbook. Oxford: Pergamon Press; 1988.
[17] Timoshenko SP, Goodier JN. Theory of elasticity. 3rd ed. New York: McGraw-Hill; 1970.
[18] Camponovo C, Schweizer J. Ann Glaciol 2001;32:44.
[19] Kirchner HOK, Michot G, Narita H, Suzuki T. Phil Mag A 2001;81:2161.
[20] Petrenko VF, Withworth RW. Physics of ice. Oxford: University Press; 1999.
[21] Schweizer J. Cold Reg Sci Technol 1999;30:43.
[22] Louchet F. 2001, private communication.